

TABLE OF CONTENTS

	Page	
NOTATION	v	1/A7
SUMMARY	1	1/A8
INTRODUCTION	1	1/A8
THEORY	2	1/A9
General Takeoff Solution	2	1/A9
Noise contour-	2	1/A9
Contour area-	8	1/B1
Contour extremity-	11	1/B4
General Landing Solution	11	1/B4
SUMMARY OF EQUATIONS	12	1/B5
CALCULATOR IMPLEMENTATION	13	1/B8
EXAMPLE CONTOURS	16	1/B9
APPLICATION TO JET STOL FLIGHT PATH	17	1/B10
CONCLUDING REMARKS	19	1/B12
REFERENCES	19	1/B12
FIGURES	21	1/B14

DEM 830-H-15

NAS 1.60:1432

REC 4 1979

NASA Technical Paper 1432

COMPLETED

A Closed-Form Solution for Noise Contours

Elwood C. Stewart and Thomas M. Carson

NOVEMBER 1979

NASA

NASA Technical Paper 1432

A Closed-Form Solution for Noise Contours

9519 1-13
Elwood C. Stewart and Thomas M. Carson
Ames Research Center
Moffett Field, California



National Aeronautics
and Space Administration

Scientific and Technical
Information Branch

1979

Blank Page

TABLE OF CONTENTS

	<u>Page</u>
NOTATION	v
SUMMARY	1
INTRODUCTION	1
THEORY	2
General Takeoff Solution	2
Noise contour-	2
Contour area-	8
Contour extremity-	11
General Landing Solution	11
SUMMARY OF EQUATIONS	12
CALCULATOR IMPLEMENTATION	15
EXAMPLE CONTOURS	16
APPLICATION TO JET STOL FLIGHT PATH	17
CONCLUDING REMARKS	19
REFERENCES	19
FIGURES	21

Blank Page

NOTATION

AB	distance from end of runway to touchdown, m
AC	distance from end of runway to start of takeoff roll, m
L_{RW}	runway length, m
ℓ_n	direction cosine of nth segment in horizontal plane
R	slant range from aircraft to observer, m
s_n	length of nth segment in horizontal plane, m
U	position vector $(u \ v \ w)^T$, m
X	position vector $(x \ y)^T$, m
X'	position vector $(x' \ y')^T$, m
X''	position vector $(x'' \ y'')^T$, m
\mathcal{X}	position vector $(x' \ y' \ z')^T$, m
x'_{nf}	final coordinate of nth segment, m
x'_{ni}	initial coordinate of nth segment, m
γ	flight-path angle between velocity vector and horizontal plane, deg
Δ	translation transformation from x'', y'' to x, y coordinate system
θ	change in heading angle between segments (positive clockwise or to the right), deg
Λ	rotation transformation from x'', y'' to x', y' coordinate system
ψ	heading angle, angle between the x axis in horizontal plane and projection of V in horizontal plane (positive counterclockwise), deg
Ω	transformation from u, v, w to x', y', z' coordinate system

A CLOSED-FORM SOLUTION FOR NOISE CONTOURS

Elwood C. Stewart and Thomas M. Carson

Ames Research Center

SUMMARY

In this report is described an analytical approach for generating noise contours that overcomes the difficulties of existing programs. Although many noise-contour programs are available, they require large computers and a sustained major effort for use, are complex and slow, and are generally not desirable for interactive use for on-line piloted-simulator use. The method developed here is valid for arbitrarily complex paths and reveals the importance of various factors that influence contour shape and size. The calculations are simple enough to be implemented on a small, hand-held programmable calculator, and a program for the HP-67 calculator is illustrated. The method is fast, simple, and gives the area, the contour, and its extremities for arbitrary flight paths for both takeoffs and landings.

INTRODUCTION

Noise impact on the community is one of the most serious problems of aircraft operations. The importance of this problem has been highlighted by the increased public concern with environmental issues. To deal with the problem, NASA is engaged in research on technical approaches for noise reduction applicable to new aircraft.

A key tool in the study of noise impact has been noise-contour calculation programs, a number of which have been developed over the last 10 years (e.g., refs. 1-3). These programs and their many modifications have been widely used by the Government and by industry. The programs handle very general situations which can include excess ground attenuation, shielding, multiple flights, and various mixes of aircraft. However, there are many difficulties in the use of these programs. First of all, the programs are generally large and not well documented. Consequently, they require extensive study to operate. Second, the programs are difficult to make operational, especially if they have been stored for a long time. As a consequence of these two difficulties, the successful use of these programs usually requires a large and sustained commitment. Third, the programs require a large computer and it is often difficult to obtain sufficient time on a large computer for use in an interactive manner. Further, the programs are slow in operation. And finally, the programs are generally not desirable for on-line use with piloted simulators because of their size and slowness. For these reasons, another method that generates noise contours much more rapidly and simply, and one that utilizes minimum computational facilities is desirable.

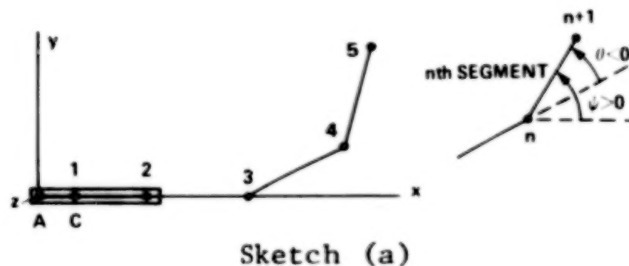
The present report is concerned with a closed-form analytical approach for calculating noise contours that overcomes the difficulties just discussed.

As is common with most noise programs, an isotropic noise source is assumed, although it is believed the present approach is extendable to an anisotropic noise source. The method is valid for arbitrarily complex flight paths. For simple paths, the calculations can be accomplished by hand; for complex paths, the calculations are best done on a small hand-held calculator with programming capability, such as the HP-67. The analysis reveals the fundamental nature of the contours and the importance of the various factors that influence its shape and size. The method is fast, simple, and gives the area, the actual contour, and its extremities for arbitrarily complex flight paths for both takeoffs and landings.

THEORY

General Takeoff Solution

In this section we will consider the noise impact for an aircraft flying a takeoff trajectory. A typical three-dimensional trajectory consisting of straight-line segments is illustrated by the plan view in sketch (a) below.

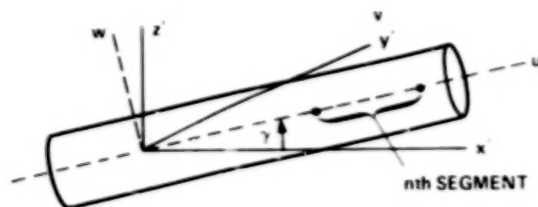


Here, way-point 1 is the start of the takeoff roll located a distance AC from the origin, way-point 2 is lift-off, and the general n th segment is between the n th and $(n+1)$ way points, as indicated. Each segment is characterized by: (1) an angle ψ measured positive counterclockwise from the x axis to the segment or, alternatively, by an angle θ measuring the incremental change in heading between segments, positive to the right or clockwise so as to correspond with existing nomenclature in contour programs (see p. 5 of ref. 4); (2) an inclination angle γ measured positive above the horizontal; (3) a segment length s ; and (4) a distance R from the aircraft corresponding to the desired EPNdB noise contour and specified thrust level.

In the following paragraphs interest will focus on determining the noise contour, the contour area, and the extremity of the contour, that is, where the end of the contour is located.

Noise contour- The noise contour will be composed of contributions due to each of the various segments, and the various pieces of the contour must be determined and suitably pieced together so as to generate the complete contour. For this purpose, consider the path of the aircraft along the n th segment in sketch (b). The aircraft, when represented by an isotropic noise source, will generate a constant noise-level surface in the shape of a

cylinder as indicated by the following sketch (b). Now define the orthogonal coordinate system u, v, w such that the u axis is aligned with the n th segment and the origin is located at the intersection of the u axis and the horizontal plane, and the v axis lies in the horizontal plane as shown in sketch (b). Another orthogonal coordinate system x', y', z' with the same origin is shown in which x' is the projection of the u axis on the horizontal plane, and the y' axis is coincident with the v axis.



Sketch (b)

The equation for a general quadric is

$$U^T \mathcal{Q} U = R^2 \quad (1)$$

where $U = (u \ v \ w)^T$. For a cylinder aligned with the u axis,

$$\mathcal{Q} = \begin{bmatrix} 0 & 0 & 0 \\ 0 & 1 & 0 \\ 0 & 0 & 1 \end{bmatrix} \quad (2)$$

If we define $\mathcal{X} = (x' \ y' \ z')^T$, the transformation between two vectors \mathcal{X} and U is

$$\mathcal{X} = \Omega U \quad (3)$$

where Ω is an orthogonal matrix given by

$$\Omega = \begin{bmatrix} \cos \gamma & 0 & -\sin \gamma \\ 0 & 1 & 0 \\ \sin \gamma & 0 & \cos \gamma \end{bmatrix} \quad (4)$$

Thus equation (1), when transformed by equation (3), gives

$$\mathcal{X}^T \Omega \mathcal{Q} \Omega^T \mathcal{X} = R^2 \quad (5)$$

where

$$\Omega\Omega^T = \begin{bmatrix} \sin^2 \gamma & 0 & -\sin \gamma \cos \gamma \\ 0 & 1 & 0 \\ -\sin \gamma \cos \gamma & 0 & \cos^2 \gamma \end{bmatrix} \quad (6)$$

Equation (5) is a quadric equation for the three-dimensional noise contour for a given noise level in terms of the x', y', z' coordinate system.

The intersection of this surface with the horizontal plane will give the noise contour. A plane is represented by:

$$m^T \mathcal{X} = k \quad (7)$$

where $m = (m_1 \ m_2 \ m_3)^T$, and k is a constant. For the horizontal ground-level plane,

$$\left. \begin{aligned} m^T &= (0 \ 0 \ m_3) \\ k &= 0 \end{aligned} \right\} \quad (8)$$

Since \mathcal{X} is orthogonal to m , it is given by

$$\mathcal{X} = (x' \ y' \ 0)^T \quad (9)$$

The contour can now be obtained by determining the intersection of equations (5) and (9). Partition the following matrices as shown,

$$\Omega\Omega^T = \left[\begin{array}{cc|c} \sin^2 \gamma & 0 & -\sin \gamma \cos \gamma \\ 0 & 1 & 0 \\ \hline -\sin \gamma \cos \gamma & 0 & \cos^2 \gamma \end{array} \right] \equiv \begin{bmatrix} A & B \\ C & D \end{bmatrix} \quad (10)$$

$$\mathcal{X} = \begin{bmatrix} x' \\ y' \\ 0 \end{bmatrix} \equiv \begin{bmatrix} X' \\ 0 \end{bmatrix} \quad (11)$$

and substitute these two matrices in equation (5) to obtain

$$X'^T A X' = R^2 \quad (12)$$

where

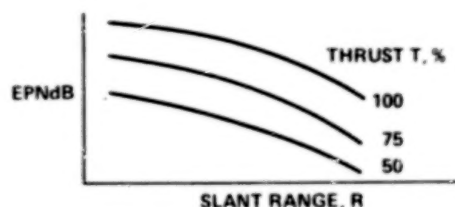
$$X' = \begin{bmatrix} x' \\ y' \end{bmatrix} \quad (13)$$

$$A = \begin{bmatrix} \sin^2 \gamma & 0 \\ 0 & 1 \end{bmatrix} \quad (14)$$

Equation (12) represents a conic section. Because the diagonal elements in equation (14) are greater than zero, equation (12) can be recognized as an ellipse. Note that only two parameters, γ and R , are required to define the contour.

It should be pointed out that the form of equation (12) applies to each segment, although the two constants may differ on each segment. Further, it is clear that each segment contributes only a portion of its conic section to the total contour. This portion and the way the various portions are to be pieced together will be discussed in a few paragraphs.

The value of R can be determined from the basic noise-source data which are typically given as a function of two variables, the slant range R and thrust level T , as illustrated in sketch (c). The value of R is determined



Sketch (c)

directly from these data for any desired EPNdB contour and for any value of thrust T . This latter value could be estimated, determined from flight data, or determined from a control generator as described in reference 4.

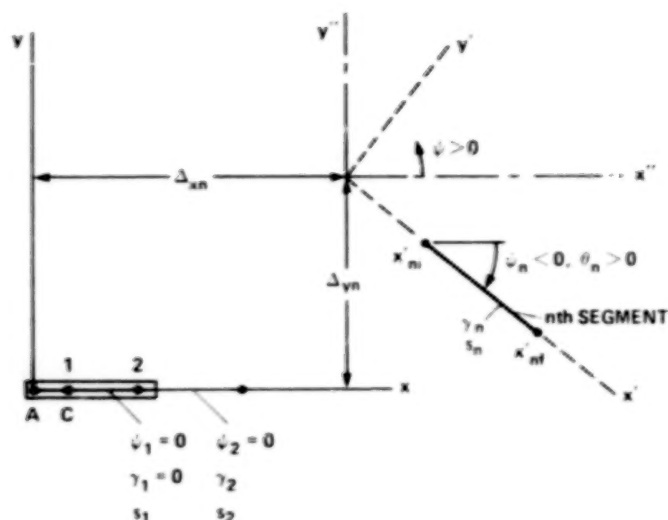
An example of special interest is a flight path consisting of only one segment at a constant flight-path angle as indicated in sketch (b). The contour in this case is given by equation (12) as

$$y' = \sqrt{R^2 - (x')^2 \sin^2 \gamma} \quad (15)$$

For a given R and γ , this equation can be plotted directly as function of x' . The maximum dimensions of the contour are obviously

$$\left. \begin{aligned} x'_{\max} &= \frac{R}{\sin \gamma} \\ y'_{\max} &= \pm R \end{aligned} \right\} \quad (16)$$

Now we will consider how to obtain the total contour by properly combining the contributions of the various segments. The situation is illustrated in sketch (d) which is an elaboration of sketch (a). Recall that the contour



Sketch (d)

in the x', y' coordinate system is given by equation (12). This equation must be transformed to the x, y coordinate system, in common with each of the other segments. This is done by rotation and translation transformations. As for rotation, the transformation is

$$X' = \Lambda_n X'' \quad (17)$$

where the vector X'' is defined by the coordinate system shown in sketch (d), Λ_n is an orthogonal matrix given by

$$\Lambda_n = \begin{bmatrix} \cos \psi_n & \sin \psi_n \\ -\sin \psi_n & \cos \psi_n \end{bmatrix} \quad (18)$$

and ψ_n is defined by

$$\psi_n = -\sum_{i=1}^n \theta_i \quad (19)$$

in accordance with discussion following sketch (a). Thus, combining equations (12) and (17) we obtain

$$X''^T \Lambda_n^T A_n \Lambda_n X'' = R_n^2 \quad (20)$$

As for translation, the transformation is

$$X = X'' + \Delta_n \quad (21)$$

where

$$\Delta_n = \begin{bmatrix} \Delta x_n \\ \Delta y_n \end{bmatrix} \quad (22)$$

Combining equations (20) and (21) we obtain

$$(X - \Delta_n)^T \Lambda_n^T A_n \Lambda_n (X - \Delta_n) = R_n^2 \quad (23)$$

This is the equation of the contour generated by an aircraft flying along the extended n th segment in terms of the basic x, y coordinate system. Note that this equation applies to each segment but that the parameters for each segment may be different. Also note that in addition to the parameters γ and R , previously discussed with equation (12), there are now two more quantities, Δ and Λ , involved.

Now we will determine some of the quantities that are needed in equation (23). First, is the matrix $\Lambda_n^T A_n \Lambda_n$; it can be shown from equations (14) and (18) that

$$\Lambda_n^T A_n \Lambda_n = \begin{bmatrix} a_n & b_n \\ b_n & d_n \end{bmatrix} \quad (24)$$

where

$$\left. \begin{aligned} a_n &= 1 - \cos^2 \psi_n \cos^2 \gamma_n \\ b_n &= -\sin \psi_n \cos \psi_n \cos^2 \gamma_n \\ d_n &= 1 - \sin^2 \psi_n \cos^2 \gamma_n \end{aligned} \right\} \quad (25)$$

Second, is the vector Δ_n which is determined as follows: Let n be the segment between the n th and $(n+1)$ way points, let s_n be the segment length in the horizontal plane, and let ℓ_n be its direction cosine matrix:

$$\ell_n = \begin{bmatrix} \cos \psi_n \\ \sin \psi_n \end{bmatrix} \quad (26)$$

where ψ_n is measured positive counterclockwise from the x'' axis to the segment as discussed previously following figure 1. Now, from sketch (d) it can be shown that for the n th segment

$$\Delta_n = \sum_{k=1}^{n-1} l_k s_k - \frac{l_n}{\tan \gamma_n} \sum_{k=1}^{n-1} s_k \tan \gamma_k + \begin{bmatrix} AC \\ 0 \end{bmatrix} \quad (27)$$

The only other variable in equation (23) is R which has been previously discussed.

Equation (23) can be put in a form more suitable for computation. Since

$$X - \Delta_n = \begin{bmatrix} x - \Delta_{xn} \\ y - \Delta_{yn} \end{bmatrix} \quad (28)$$

equation (23) can be shown to reduce to

$$a_n(x - \Delta_{xn})^2 + 2b_n(x - \Delta_{xn})(y - \Delta_{yn}) + d_n(y - \Delta_{yn})^2 = R^2 \quad (29)$$

This is the equation for the contour in a useful computational form. For any given choice of x , the corresponding value of y is readily obtained as the solution of a quadratic equation in $y - \Delta_{yn}$. It should be noted that for a given choice of x , the parameters in equation (29) should correspond to the segment closest to x . The appropriate segment can be determined by examining the geometry of the situation. Or, it can be implemented more precisely as follows. Determine the beginning x_{ni} and the end x_{nf} of the n th segment by

$$x_{ni} = AC + \sum_{k=1}^{n-1} s_k \cos \psi_k \quad (30)$$

$$x_{nf} = AC + \sum_{k=1}^n s_k \cos \psi_k \quad (31)$$

Then the n th segment to use must be the one such that

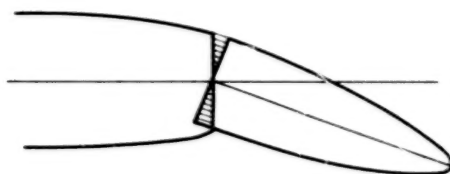
$$x_{ni} < x < x_{nf} \quad (32)$$

Obviously the x values need not exceed x_{max} , the value of which will be discussed in a later section.

Contour area- The contour area will be composed of contributions due to each of the various segments of the flight path. The first segment, which is on the ground (sketch (d)) has an area given by

$$A_1 = 2R_1 s_1 + \frac{\pi R_1^2}{2} \quad (33)$$

The remaining segments are all above the ground, and it will be necessary to consider the area contributed by any individual n th segment. An approximation is made here that the total contour of an arbitrary path is the same as if the trajectory is "straightened out" so that it lies in one vertical plane. As illustrated in sketch (e), this procedure of straightening out the



Sketch (e)

trajectory amounts to assuming the two cross-hatched areas are equal. It is clear that this approximation becomes worse as the differences between consecutive ψ become large. Even then, however, the error is generally only a small portion of the total contour area so that the approximation is generally very good.

Consider now the area contributed by the n th segment illustrated in sketch (d). The area between any two points denoted by lower limit LL and upper limit UL is given by

$$A_n(LL, UL) = 2 \int_{LL}^{UL} y' dx' \\ = \left[x' \sqrt{R_n^2 - (x')^2 \sin^2 \gamma_n} + \frac{R_n^2}{\sin \gamma_n} \sin^{-1} \frac{x' \sin \gamma_n}{R_n} \right]_{LL}^{UL} \quad (34)$$

where equation (15) has been utilized. This equation applies to each segment that is in the air, and the quantities R_n and γ_n are known for each of these segments. The limits, however, need some careful consideration.

For the special case of only two segments, the area due to the second segment (i.e., the straight-line segment at a nonzero flight-path angle) is obtained by putting $LL = 0$ and $UL = x'_{\max}$ as given by equation (16). The result is

$$A_2(0, x'_{\max}) = \frac{\pi R_2^2}{2 \sin \gamma_2} \quad (35)$$

This is the total contour area due to the second segment.

Consider now the determination of the limits LL and UL in equation (34) for the area due to the general n th segment. Let L_n be the length of the contour under the assumption that the aircraft continues to fly the extension of the n th segment. From equation (16), L_n is

$$L_n = \frac{R_n}{\sin \gamma_n} \quad (36)$$

Recalling that the origin of the x', y' coordinate system in sketch (d) was determined by the intersection of the extension of the n th segment and the horizontal plane, we can deduce that the beginning and end of the n th segment are given, respectively, by

$$x'_{ni} = \frac{\sum_{k=1}^{n-1} s_k \tan \gamma_k}{\tan \gamma_n} \quad (37)$$

$$x'_{nf} = x'_{ni} + s_n \quad (38)$$

Then it is clear that

$$\begin{aligned} LL &= x'_{ni} \\ UL &= \left\{ \begin{array}{ll} x'_{nf} & \text{if } L_n > x'_{nf} \quad (\text{contour not ended}) \\ L_n & \text{if } L_n < x'_{nf} \quad (\text{contour ended and } n \text{ is the last segment}) \end{array} \right\} \end{aligned} \quad (39)$$

In the first case, the end of the contour has not been reached by the end of the n th segment, while in the second case it has. Then the area contributed by the n th segment is

$$\begin{aligned} A_n &= \left[x' \sqrt{R_n^2 - (x')^2 \sin^2 \gamma_n} + \frac{R_n^2}{\sin \gamma_n} \sin^{-1} \frac{x' \sin \gamma_n}{R_n} \right]_{x'_{ni}}^{UL} \\ &\equiv \left[F \right]_{x'_{ni}}^{UL} \end{aligned} \quad (40)$$

where F is the quantity in the brackets. This expression is valid for all segments including the last one. However, on the last segment, certain round-off errors may occur that cause complications in using equation (40). Thus, it is usually better to use an alternative expression that avoids this problem for the area due to the last segment:

$$A_N = \frac{\pi R_n^2}{2 \sin \gamma_n} - \left[F \right]_0^{x'_{ni}} \quad (41)$$

Another way to avoid problems due to round-off errors is to slightly reduce the upper limit in equation (40) on the last segment.

The total area of the contour due to the total of N segments is now given by:

$$A_T = A_1 + \sum_{n=2}^N \left[F \right]_{x'_{ni}}^{UL} \quad (42)$$

Contour extremity - The end of the contour is of special interest, and it can be readily determined from the equations already given. From the last section, on the last segment,

$$\left. \begin{aligned} x'_{\max} &= L_n \\ y'_{\max} &= 0 \end{aligned} \right\} \quad (43)$$

Then using the transformations in equations (17) and (21)

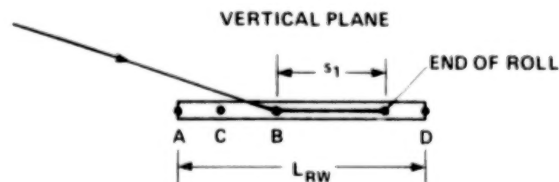
$$\begin{aligned} X_{\max} &= X'_{\max} + \Delta_n \\ &= \Lambda_n^T X'_{\max} + \Delta_n \end{aligned} \quad (44)$$

Thus

$$\begin{bmatrix} x_{\max} \\ y_{\max} \end{bmatrix} = \begin{bmatrix} \cos \psi_n & -\sin \psi_n \\ \sin \psi_n & \cos \psi_n \end{bmatrix} \begin{bmatrix} x'_{\max} \\ 0 \end{bmatrix} + \begin{bmatrix} \Delta_{xn} \\ \Delta_{yn} \end{bmatrix} \quad (45)$$

General Landing Solution

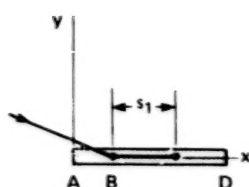
Landing problems can be solved by transforming them to equivalent takeoff problems. The landing situation is shown in the vertical plane in sketch (f),



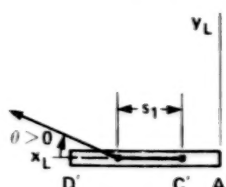
Sketch (f)

here B is the touchdown point and s_1 is the length of the ground-roll segment, at the end of which the aircraft has stopped. Now, make the following set of transformations illustrated below by the plan views (sketches

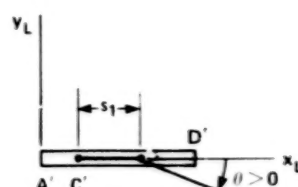
HORIZONTAL PLANES



Sketch (g)



Sketch (h)



Sketch (i)

(g)-(i)). Sketch (g) illustrates a landing situation in the given coordinate system. In sketch (h), the direction of the flight has been reversed and the origin and direction of the x axis has been changed. The variables are denoted by x_L and y_L . Also, the labeling of the points A' , C' , and D' corresponds to this new takeoff problem. From this sketch it can be seen that

$$A'C' = L_{RW} - AB - s_1 \quad (46)$$

and $A'C'$ is the variable now used in the equivalent takeoff problem. Also,

$$x_L = L_{RW} - x \quad (47)$$

Finally, in sketch (i), the entire diagram has been rotated clockwise by π and the direction of the y_L axis reversed. This has maintained the relationship between the flight path and the coordinate axes. Then we have

$$y_L = -y \quad (48)$$

Now the problem can be solved in the form shown in sketch (i) as a takeoff problem. We need to use the value $A'C'$ in this equivalent takeoff problem, and to order the segments in sketch (h) or (i) as a takeoff problem starting from C' . Also note that θ is measured positive clockwise so that it can be determined directly from sketch (h) if desired. The takeoff equations previously developed apply directly using x_L and y_L as the variables instead of x and y . Finally, the contour in terms of x_L and y_L is converted to the variables x and y in the original coordinate system by equations (47) and (48). The extremity of the contour x_{Lmax} is transformed by these same equations.

SUMMARY OF EQUATIONS

In this section we merely collect the previous equations and procedures for determining contour areas, extremities of the contour, and the contour itself for both landings and takeoffs.

○ Takeoffs

• Area

Segment 1

$$A_1 = -\frac{\pi R_1^2}{2} + 2R_1 s_1$$

Segment n for $n \geq 2$

$$L_n = \frac{R_n}{\sin \gamma_n}$$

$$x'_{ni} = \frac{\sum_{k=1}^{n-1} s_k \tan \gamma_k}{\tan \gamma_n}$$

$$x'_{nf} = x'_{ni} + s_n$$

$$UL = \begin{cases} x'_{nf} & \text{if } L_n > x'_{nf} \Rightarrow \text{contour not ended} \\ L_n & \text{if } L_n < x'_{nf} \Rightarrow \text{contour ended, and } n \\ & \text{is the last segment} \end{cases}$$

$$A_n = \left[x' \sqrt{R_n^2 - (x')^2 \sin^2 \gamma_n} + \frac{R_n^2}{\sin \gamma_n} \sin^{-1} \frac{x' \sin \gamma_n}{R_n} \right]_{x'_{ni}}^{UL}$$

$$= \left[F \right]_{x'_{ni}}^{UL}$$

where F is defined as the quantity in the brackets. For the last segment, one can use

$$A_N = \frac{\pi R_n^2}{2 \sin \gamma_n} - \left[F \right]_0^{x'_{ni}}$$

• Extremity of contour

For last segment, $L_n < x'_{nf}$

Set

$$x'_{\max} = L_n$$

Then

$$X_{\max} = \begin{bmatrix} x_{\max} \\ y_{\max} \end{bmatrix} = \Lambda^T \begin{bmatrix} x'_{\max} \\ 0 \end{bmatrix} + \begin{bmatrix} \Delta_{xn} \\ \Delta_{yn} \end{bmatrix}$$

where

$$\Delta_n = \begin{bmatrix} \Delta_{xn} \\ \Delta_{yn} \end{bmatrix} = \sum_{k=1}^{n-1} \ell_k s_k - \frac{\ell_n}{\tan \gamma_n} \sum_{k=1}^{n-1} s_k \tan \gamma_k + \begin{bmatrix} AC \\ 0 \end{bmatrix}$$

$$\ell_n = \begin{bmatrix} \cos \psi_n \\ \sin \psi_n \end{bmatrix}$$

$$\psi_n = - \sum_{i=1}^n \theta_i$$

$$\Lambda_n = \begin{bmatrix} \cos \psi_n & \sin \psi_n \\ -\sin \psi_n & \cos \psi_n \end{bmatrix}$$

• Contour equations ($n \geq 2$)

Choose $x \leq x_{\max}$

Compute $x'' = x - \Delta_{xn}$

Then compute y'' from

$$a_n (x'')^2 + 2b_n (x'')(y'') + d_n (y'')^2 = R_n^2$$

where

$$a_n = 1 - \cos^2 \psi_n \cos^2 \gamma_n$$

$$b_n = -\sin \psi_n \cos \psi_n \cos^2 \gamma_n$$

$$d_n = 1 - \sin^2 \psi_n \cos^2 \gamma_n$$

Then

$$y = y'' + \Delta_{yn}$$

(For $n = 1$ and $x_{1i} < x < x_{1f}$, $y = \pm R_1$)

The choice of x and the parameters for the n th segment must satisfy

$$x_{ni} < x < x_{nf}$$

where

$$x_{ni} = AC + \sum_{k=1}^{n-1} s_k \cos \psi_k$$

$$x_{nf} = AC + \sum_{k=1}^n s_k \cos \psi_k$$

○ Landings

- Contour

Let x_L and y_L replace x and y in the takeoff equations

Let $A'C' = L_{RW} - AB - s_i$

Choose x

Compute $x_L = L_{RW} - x$

Compute y_L from takeoff equations

Compute $y = -y_L$

- Extremity of contour

$$X_{\max} = \begin{bmatrix} L_{RW} \\ 0 \end{bmatrix} - X_{L\max}$$

CALCULATOR IMPLEMENTATION

The equations for the relevant characteristics of the noise contours can be implemented on a small hand-held programmable calculator. In this way the necessity to access a large central computer system is avoided. In this section we describe the implementation of the contour calculations for one of the common programmable calculators, the Hewlett-Packard HP-67.

Because of the limitation of programming memory in the HP-67, the program was accomplished in two parts: the contour-area and the contour-plotting programs.

The area program calculates and sums the area of the noise contour due to each segment and also calculates some quantities necessary for determining the noise contour. The contour-plotting program determines the y values of the contour associated with an input value x . Instructions for using each of these programs are given in figures 1 and 2 for takeoffs and landings. Some discussion of the combined use of the two programs is required because there

are two possible options. The first option, illustrated in figure 3(a), is used when the number of segments in the flight path is four or less. The area program must be run first because it calculates quantities that are required by the contour-plotting program. Next, the contour-plotting program is loaded and the contour is plotted. The second option, illustrated in figure 3(b), is the more general case. It must be used when the flight path consists of more than four segments; it can also be used when the user wants to postpone plotting the contour to a later time regardless of the number of segments. With this option, after the area program calculations have been completed for the first four segments, the area and the intermediate quantities are written on a magnetic card. The user then goes back to repeat the procedure with more segments until the complete flight path is finished. Later, when it is desired to plot the contour, the contour-plotting program and the intermediate quantities previously computed are loaded in the calculator and the contour is plotted.

For those interested in the details of the program, a flow chart and a listing of the area program are given in figures 4 and 5, respectively; figures 6 and 7 provide the same information for the plotting program.

EXAMPLE CONTOURS

In this section several example applications of the preceding noise-contour method are given and compared with the exact results obtained from a large contour program (refs. 1-3) using an IBM-360 computer.

All of the examples to be discussed are based on the same aircraft for reasons of simplicity. We will use a typical current conventional jet transport aircraft that was used in the study of reference 4. The noise characteristics for this aircraft are reproduced in figure 8; linear interpolation is used for intermediate thrust values. Six examples have been chosen so as to exercise many of the possibilities that can arise. The first three examples are takeoffs; they and the defining data are illustrated in figure 9. The last three examples are landings as illustrated in figure 10. The variables s , γ , and θ were chosen for desired geometry while R was determined from the noise curve in figure 8 for the given thrust level.

The contours for the examples are shown in figures 11 through 15. Ground attenuation and shielding have been omitted from these examples. Data from two sources are shown. The first source of data was obtained from the IBM-360 program and is illustrated by the contours. The program is about 100,000 bytes (8 bit words) in size, and a substantial amount of time and effort was required to obtain these results. The second source of data was obtained from the closed-form solution using the HP-67 calculator and is illustrated by the circles. Comparison of these two sets of data shows there is excellent agreement.

The contour areas for the six examples are given in the following table in which the results from the large noise contour program (IBM-360) and the

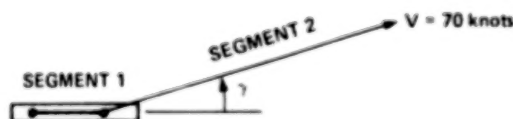
Example	Contour area, km ² (mi ²)			
	Closed-form solution		IBM-360 program	
I	154.93	(59.82)	154.9	(59.8)
II	154.93	(59.82)	155.4	(60.0)
III	100.49	(38.80)	99.5	(38.4)
IV	17.59	(6.79)	17.4	(6.7)
V	24.22	(9.35)	24.1	(9.3)
VI	154.93	(59.82)	155.4	(60.0)

closed-form solution of this report are compared. The accuracy of the closed-form solution is seen to be within 1% of the IBM-360 program results.

APPLICATION TO JET STOL FLIGHT PATH

In this section the utility of the method for examining the effect of the fundamental variables on the size of the noise contour is illustrated. For this purpose, the problem of the effect of flight-path angle γ on the size of the noise contour is studied. It can be seen that as the flight-path angle γ increases, the contour tends to become smaller from geometrical considerations. On the other hand, the increased thrust required to maintain the larger flight-path angle results in greater source noise and hence tends to enlarge the contour. These two opposing trends are examined.

The problem to be considered is shown in sketch (j), where the simple straight-line path lies in the vertical plane and the angle γ is variable.



Sketch (j)

We take an example lift-fan aircraft, the characteristics of which were summarized in reference 4. There are two state variables to this problem, γ and V , both of which are specified. The control variables are thrust, thrust angle, and angle of attack, and they are to be determined so as to achieve the specified flight path, subject to constraints on each control. This problem was considered in reference 4 where it was shown that the controls comprise a redundant set and that the redundancy can be removed by an added condition that the noise be minimized. It was also shown that the angle-of-attack constraint required for safety due to gusts was the most critical, so that a constraint $\alpha \leq 10^\circ$ was imposed. The solution given in reference 4, then, utilized the Kuhn-Tucker theory to determine the optimal set of controls subject to the angle-of-attack constraint. This same method was used for the present problem. Because of the varying flight-path angle, however, it was

necessary to impose an additional pitch-angle constraint, $\theta \leq 20^\circ$, for passenger comfort. Although the solution is obtained for all the controls, thrust is most important because it determines the source noise and hence the slant-range parameter R for the selected noise level.

The results of the calculations for a 90 EPNdB contour are shown in figure 16. Here the boundary on the control α is shown by α_{lim} such that both constraints $\alpha_{lim} \leq 10^\circ$ and $\theta_{lim} \leq 20^\circ$ are satisfied. The contour area is assumed to be due to the second segment (see sketch (j)), because the noise from the first segment is largely confined to the airport boundaries. Thus, the noise-contour area is

$$A_2 = \frac{\pi R_2^2}{2 \sin \gamma_2} \quad (51)$$

The value of R (subscripts omitted for simplicity) depends on the selected EPNdB contour (90 EPNdB in this example) and the thrust level. The thrust level T , as well as the thrust angle η , have been determined as a function of the flight-path angle γ using the method of reference 4; the results are shown in figure 16. Also shown here is the variation of the parameter R as determined from the noise data in figure 8. Finally, the contour area A of equation (51) is shown as a function of γ in figure 16.

Several interesting observations regarding these results can be made. It can be noted that T does not change greatly because the forces are balanced by a combination of small changes in T and η over the domain of γ . As a consequence, the variation of R is relatively small. Thus, the contour area varies roughly inversely with $\sin \gamma$, but increases slightly from this relationship at the large values of γ . For comparison, the inverse variation with $\sin \gamma$ is shown by the dotted curve in figure 15.

From these quantitative results, it is seen that the jet STOL aircraft, in utilizing its inherent steeper flight-path capability, produces a reduced noise-contour area with increasing flight-path angle γ because of two conflicting trends. On the one hand, the geometrical effect of a steeper path results in a reduced noise-contour area, and it is the dominant effect. On the other hand, the increased thrust required for the steeper paths causes a rather minor increase in the contour area because of the rotational degree of freedom of the thrust.

The situation would be somewhat different for a conventional jet transport airplane where there is no rotation of the thrust. In this case, the thrust must be increased linearly with γ to achieve that flight path, and that results in a nearly linear increase in R with γ . Since R enters the contour area as the second power, it can be surmised that the contour area should increase roughly linearly with γ , but with possibly some slight curvature. This trend has been verified by specific calculations for an example conventional jet transport airplane using the method of reference 4.

CONCLUDING REMARKS

The simplicity of the noise analysis presented here enables one to obtain the noise contour, its area, and its extremities for arbitrarily complex flight paths for both takeoffs and landings. The method is simple and fast, and results can be obtained either by manual calculation or by means of a small programmable calculator. The use of large programs operating on large computers is avoided. The analysis reveals the fundamental nature of the contours and the various factors that influence its size and shape.

Ground attenuation and shielding effects have been omitted from the analysis because their effects are important only on the initial portion of flight and are generally confined to the airport boundary. Analysis shows that these effects can be included if desired.

It might be noted that the single-event contour discussed herein is the obvious choice for purposes of minimizing noise impact. The impact of multiple flights can be handled by an obvious extension of the single-event results. For example, a common multiple-exposure measure, noise exposure factor (NEF), is related directly by a well-known relationship to the single-event results. Consequently, desired NEF contours can readily be generated by the present analysis.

Ames Research Center
National Aeronautics and Space Administration
Moffett Field, California 94035, April 6, 1979

REFERENCES

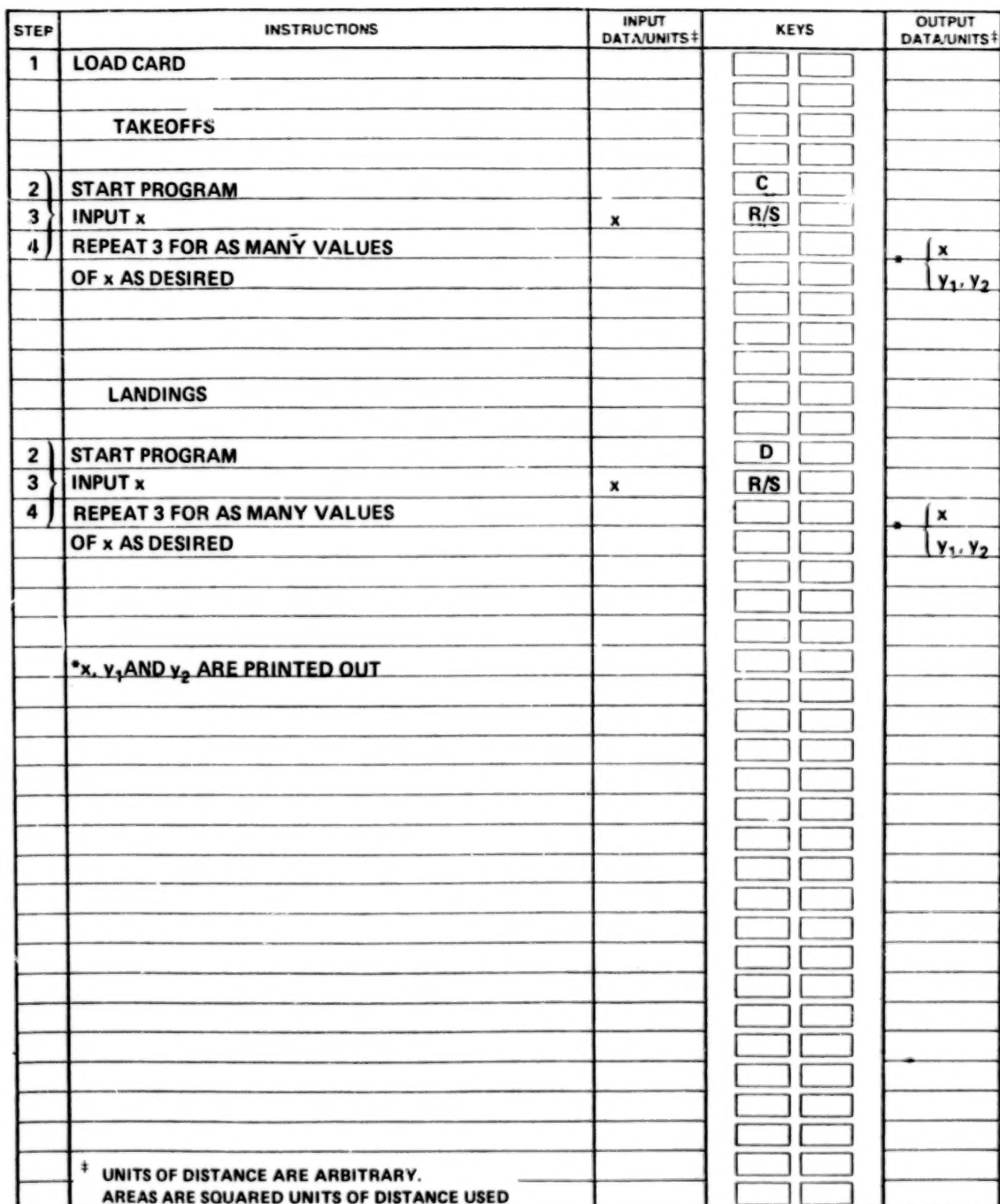
1. A Study of the Magnitude of Transportation Noise Generation and Potential Abatement, vol. III Airport/Aircraft System Noise. Serendipity, Inc., for the Department of Transportation, DOT OST-ONA-71-1, Nov. 1970.
2. Safeer, Harvey B.; and Williams, Louis J.: Airport Noise Exposure Contour Model User Manual. Department of Transportation, Rep. OST-ONA 72-3, Aug. 24, 1972.
3. The FAA Integrated Noise Model Version 1, Basic User's Guide. Federal Aviation Administration, Rep. FAA-EQ 78-01, 1978.
4. Stewart, Elwood C.; and Carson, Thomas M.: Optimal Guidance and Control for Investigating Aircraft Noise-Impact Reduction. NASA TP-1237, 1978.

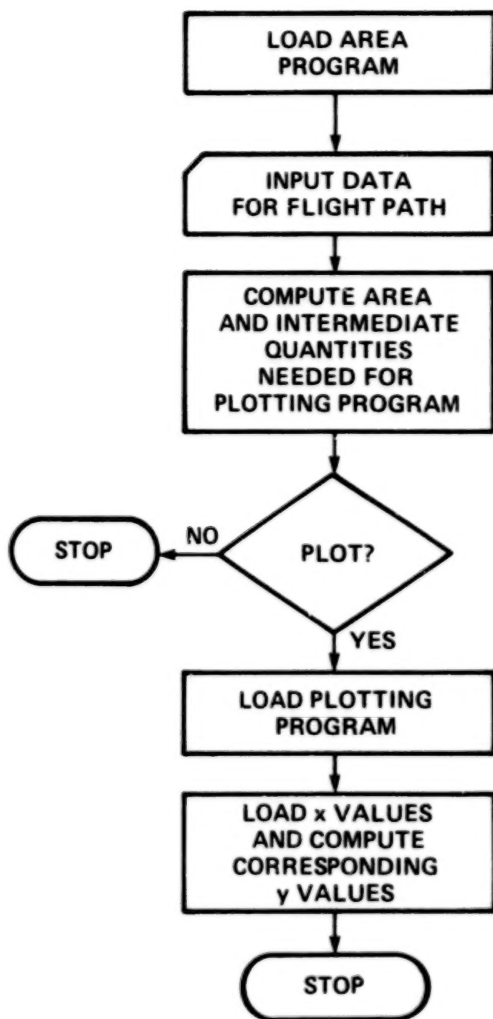
Blank Page



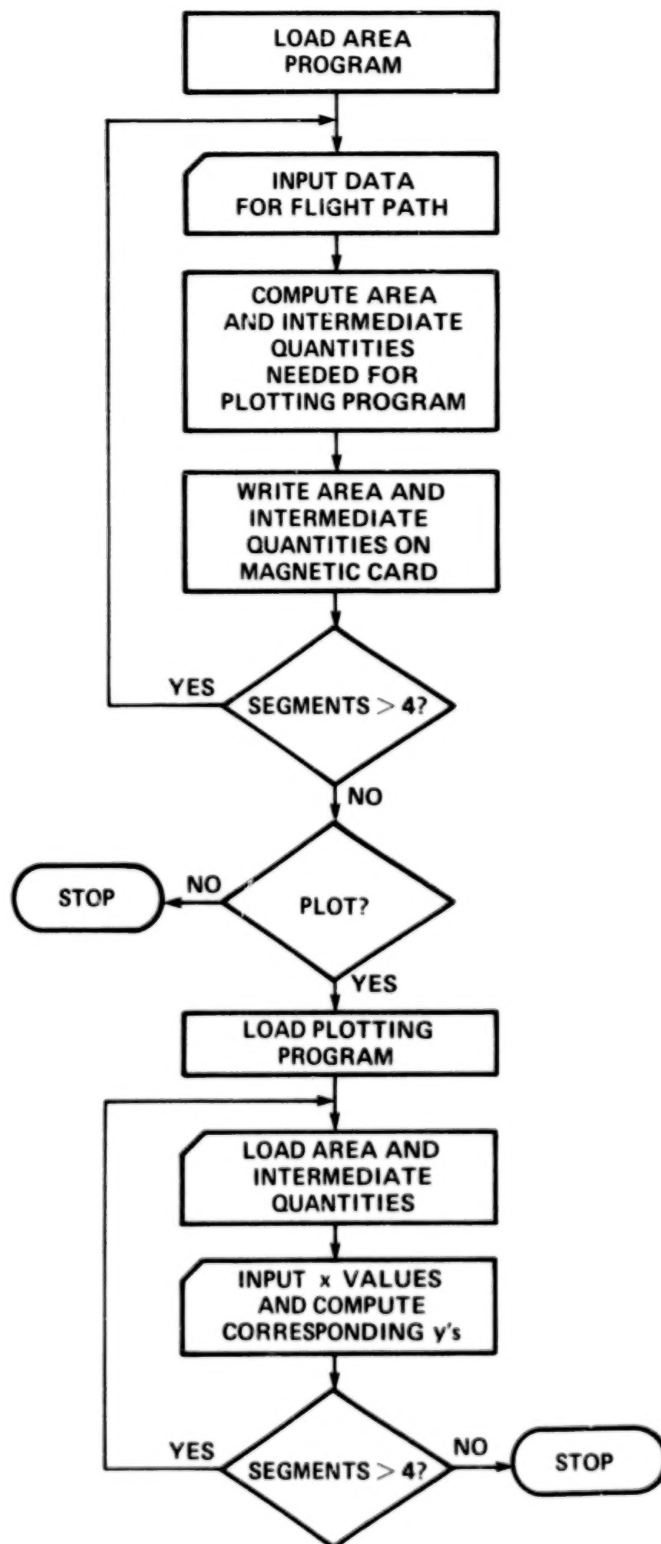
STEP	INSTRUCTIONS	INPUT DATA/UNITS†	KEYS	OUTPUT DATA/UNITS‡
1	LOAD PROGRAM CARD		<input type="text"/> <input type="text"/>	
			<input type="text"/> <input type="text"/>	
	TAKEOFFS		<input type="text"/> <input type="text"/>	
2		R_1	<input type="text"/> <input type="text"/>	
3	INPUTS FOR SEGMENT 1	s_1	<input type="text"/> <input type="text"/>	
4		AC	<input type="text"/> <input type="text"/>	A_1
	THE PROGRAM WILL STOP FOR INPUT ON SUCCEEDING SEGMENTS		<input type="text"/> <input type="text"/>	
			<input type="text"/> <input type="text"/>	
5		γ_n/deg	<input type="text"/> <input type="text"/>	$A_T = \sum_{i=1}^N A_i$
6	INPUTS FOR SEGMENT $n, n > 1$	R_n	<input type="text"/> <input type="text"/>	
7		ψ_n/deg	<input type="text"/> <input type="text"/>	y_{\max}
8		s_n	<input type="text"/> <input type="text"/>	x_{\max}
	PROGRAM RETURNS TO STEP 5 FOR INPUT ON NEXT SEGMENT		<input type="text"/> <input type="text"/>	
			<input type="text"/> <input type="text"/>	
	LANDINGS		<input type="text"/> <input type="text"/>	
			<input type="text"/> <input type="text"/>	
2		R_1	<input type="text"/> <input type="text"/>	
3	INPUTS FOR SEGMENT 1	s_1	<input type="text"/> <input type="text"/>	
4a		AB	<input type="text"/> <input type="text"/>	
4b		L_{RW}	<input type="text"/> <input type="text"/>	
	AFTER FINISHING SEGMENT 1, THE PROGRAM GOES AUTOMATICALLY TO STEP 5 ABOVE		<input type="text"/> <input type="text"/>	
			<input type="text"/> <input type="text"/>	
	* A_T IS DISPLAYED AT END OF EACH SEGMENT		<input type="text"/> <input type="text"/>	
	**PRINTED ON LAST SEGMENT		<input type="text"/> <input type="text"/>	
	CONVERSION FACTORS:		<input type="text"/> <input type="text"/>	
	$\text{mi}^2 = 3.587 \times 10^{-8} \times \text{ft}^2$		<input type="text"/> <input type="text"/>	
	$\text{km}^2 = 10^{-6} \times \text{m}^2$		<input type="text"/> <input type="text"/>	
			<input type="text"/> <input type="text"/>	
			<input type="text"/> <input type="text"/>	
			<input type="text"/> <input type="text"/>	
			<input type="text"/> <input type="text"/>	
	† UNITS OF DISTANCE ARE ARBITRARY. AREAS ARE SQUARED UNITS OF DISTANCE USED		<input type="text"/> <input type="text"/>	

Figure 1.- User instructions for contour-area program.





(a) Number of segments ≤ 4 .



(b) Delayed plotting, any number of segments.

Figure 3.- Two options for combined use of contour-area and plotting programs.

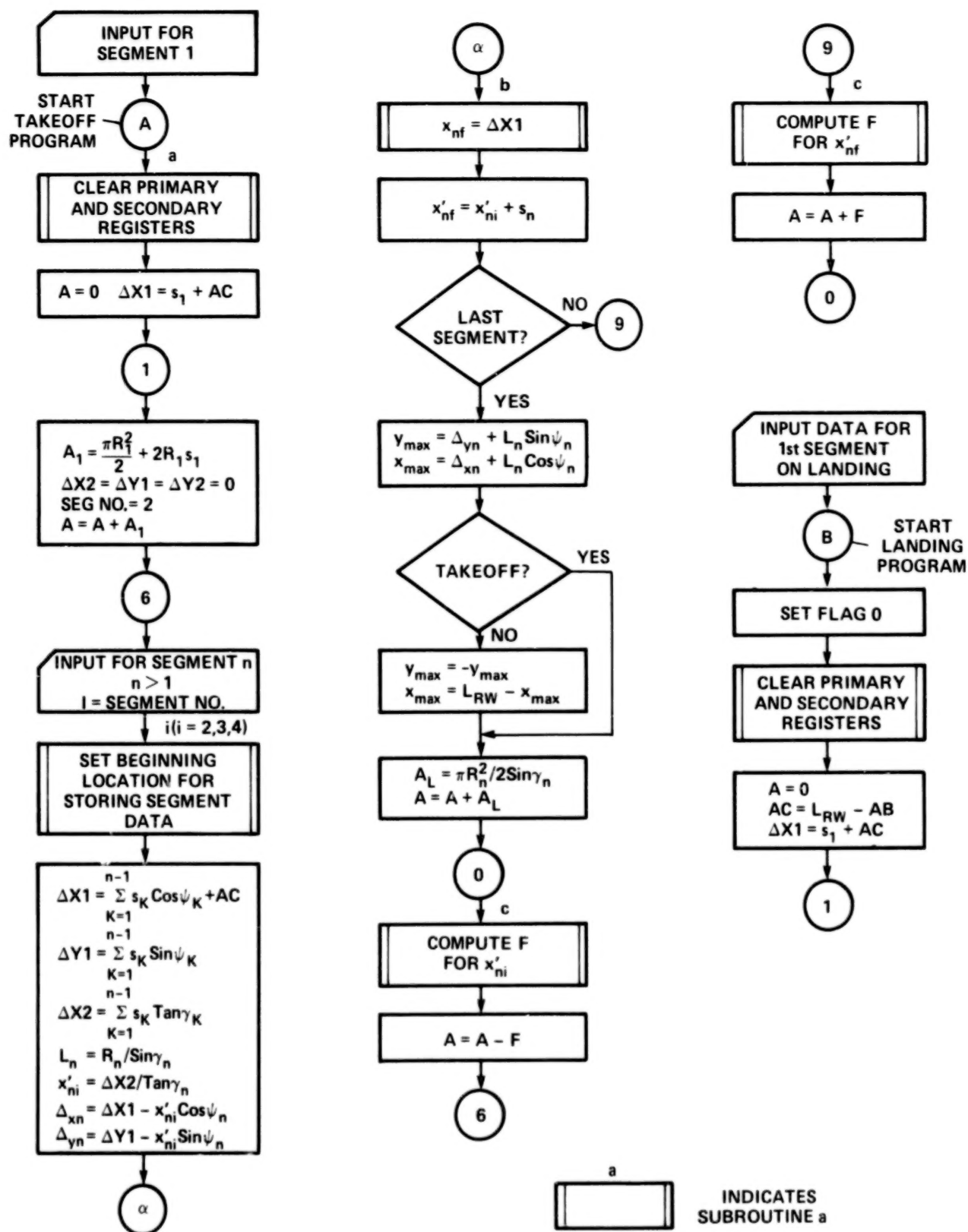


Figure 4.- Flow chart of contour-area program.

STEP	KEY ENTRY	KEY CODE	COMMENTS	STEP	KEY ENTRY	KEY CODE	COMMENTS												
001	LBLA		$\Delta X1 = \sum_{K=1}^{n-1} s_K \cos \psi_K + AC$		X		$\Delta_{xn} = \Delta X1 - x'_{ni} \cos \psi_n$												
	CF0				CHS														
	GSB _a				RCL3														
	STO3			060	+														
	R↓				ISZI														
	ST+3				STO _i														
	LBL1				RCLA														
	STO0				RCL1														
	x [→] y				SIN														
010	ENT↑				X														
	X ²		s_1		RCL5		$\Delta_{yn} = \Delta Y1 - x'_{ni} \sin \psi_n$												
	π				+														
	X				DSZI														
	2			070	DSZI														
	÷				DSZI														
	2				RCL _i														
	STOE				RCL0														
	x [→] y				X														
	R↓				ST+4														
020	X			Seg. No.		R↓			$\Delta X2 = \sum_{K=1}^{n-1} s_K \tan \gamma_K$										
	X				RCL0														
	+				RCL1														
	STO2				SIN														
	LBL6		080		X														
	DEG				ST-5														
	R/S				R↓														
	STO0				RCL1														
	R↓				COS														
	STO1				RCL0														
030	R↓		Area of seg. 1		X		$\Delta Y1 = \sum_{K=1}^{n-1} s_K \sin \psi_K$												
	RCLE				ST+3														
	STOI				R↓														
	GSB _i				RCL3														
	R↑			090	GSB _b														
	SIN				R↑														
	STOD				RCLD														
	SIN ⁻¹				RCLA														
	TAN				RCL0														
	STO _i				+														
040	ISZI		ψ_n		ISZI		$x'_{nf} = x'_{ni} + s_n$												
	R↑				ISZI														
	RCL1				ISZI														
	STO _i				ISZI														
	ISZI				ISZI														
	R↓			100	x≤y?														
	STO _i				GTO9														
	RCLD				P [→] S														
	÷				RCL9														
	STOD				P [→] S														
050	R↓		R_n		R↑		$x'_{nf} \leq L_n$ Yes : Contour not at end												
	RCL4				STO _i														
	x [→] y				R↑														
	÷				RCL1														
	STOA				SIN														
	RCL1			110	X														
	COS				-														
					F0?														
REGISTERS																			
0	s _n	1	ψ _n	2	Area	3	ΔX1	4	ΔX2	5	ΔY1	6	Tan γ ₂	7	ψ ₂	8	R ₂	9	Δ _{xn}
S0	Δ _{yn}	S1	Tan γ ₃	S2	ψ ₃	S3	R ₃	S4	Δ _{xn}	S5	Δ _{yn}	S6	Tan γ ₄	S7	ψ ₄	S8	R ₄	S9	Δ _{xn} L _{RW}
A	Δ _{yn}	x' _{ni}	B	x _{2f}	C	x _{3f}	D	L _n	E	L _{RW}	Segment No.		I						

Figure 5.- Code for contour-area program.

STEP	KEY ENTRY	KEY CODE	COMMENTS	STEP	KEY ENTRY	KEY CODE	COMMENTS
	CHS				STO9		L _{RW}
	PRTX		y _{max}	170	P _← S		
	R↑				-		
	R↑				ST-3		L _{RW} -AB
	RCL1		ψ _n		R↓		
	COS				GTO1		
	RCLD				LBL2		Set index for Seg 2
120	X				6		
	DSZ1				GTO5		Set index for Seg 3
	RCLi				LBL3		
	+		x _{max} = Δ _{xn} + L _n Cos ψ _n		1		
	GSBb			180	1		
	R↓				GTO5		
	F0?		Takeoff or landing?		LBL4		Set index for Seg 4
	-				1		
	PRTX				6		
	DSZ1				LBL5		
130	R↓				STOI		
	STOE				RTN		
	RCLi				LBLb		Set index for
	RCLD				RCLE		storing x _{max}
	π				1		for segment
	X			190	9		
	X				+		
	2				X _← 1		
	÷				R↓		
	ST+2		πR _n ² /2 Sin γ _n		STOI		
140	GTOO				R↑		
	LBL9		Setup for computing A _n		X _← 1		
	R↑				RTN		
	STOI				LBLc		
	R↓			200	÷		
	ENT↑				ENT↑		
	R↓				RAD		
	x _← y				SIN ⁻¹		
	R↑				RCLD		
	x _← y				X		
150	DSZ1				RCLi		
	DSZ1				X		
	GSBc		Evaluate F for		x _← y		
	ST+2		upper limit		X ²		
	RCLE			210	CHS		
	1				1		
	+				+		
	STOE		Increase Seg. No.		√X		
	LBL0				R↑		
	RCLA				X		
160	PCLA				RCLi		
	RCLD				X		
	GSBc		Evaluate F for x' _{ni}		+		
	ST-2				RTN		
	RCL2		Display Area	220	LBLa		Clear Primary
	GTO6				CLRG		and Secondary
	LBLB		Landing Program		P _← S		Registers
	SFO				CLRG		
	GSBa		Clear Registers		RTN		

LABELS					FLAGS	SET STATUS		
A Takeoff	B Landing	C	D	E	0 Takeoff Landing	FLAGS	TRIG	DISP
a Clear registers	b Store x _{nt} for Seg n	c Compute Δ Area	d	e	1	ON OFF		
0 Initialize Area	1 Where landing Prog. joins T.O.	2 Set Index for Seg. 2	3 Set Index for Seg. 3	4 Set Index for Seg. 4	2	0 <input type="checkbox"/> <input type="checkbox"/>	DEG <input type="checkbox"/>	FIX <input type="checkbox"/>
5 Set Index Starting Loc	6 Input for Seg. n, n > 1	7	8	9	3	1 <input type="checkbox"/> <input type="checkbox"/>	GRAD <input type="checkbox"/>	SCI <input type="checkbox"/>
						2 <input type="checkbox"/> <input type="checkbox"/>	RAD <input type="checkbox"/>	ENG <input type="checkbox"/>
						3 <input type="checkbox"/> <input type="checkbox"/>		n _____

Figure 5.- Concluded.

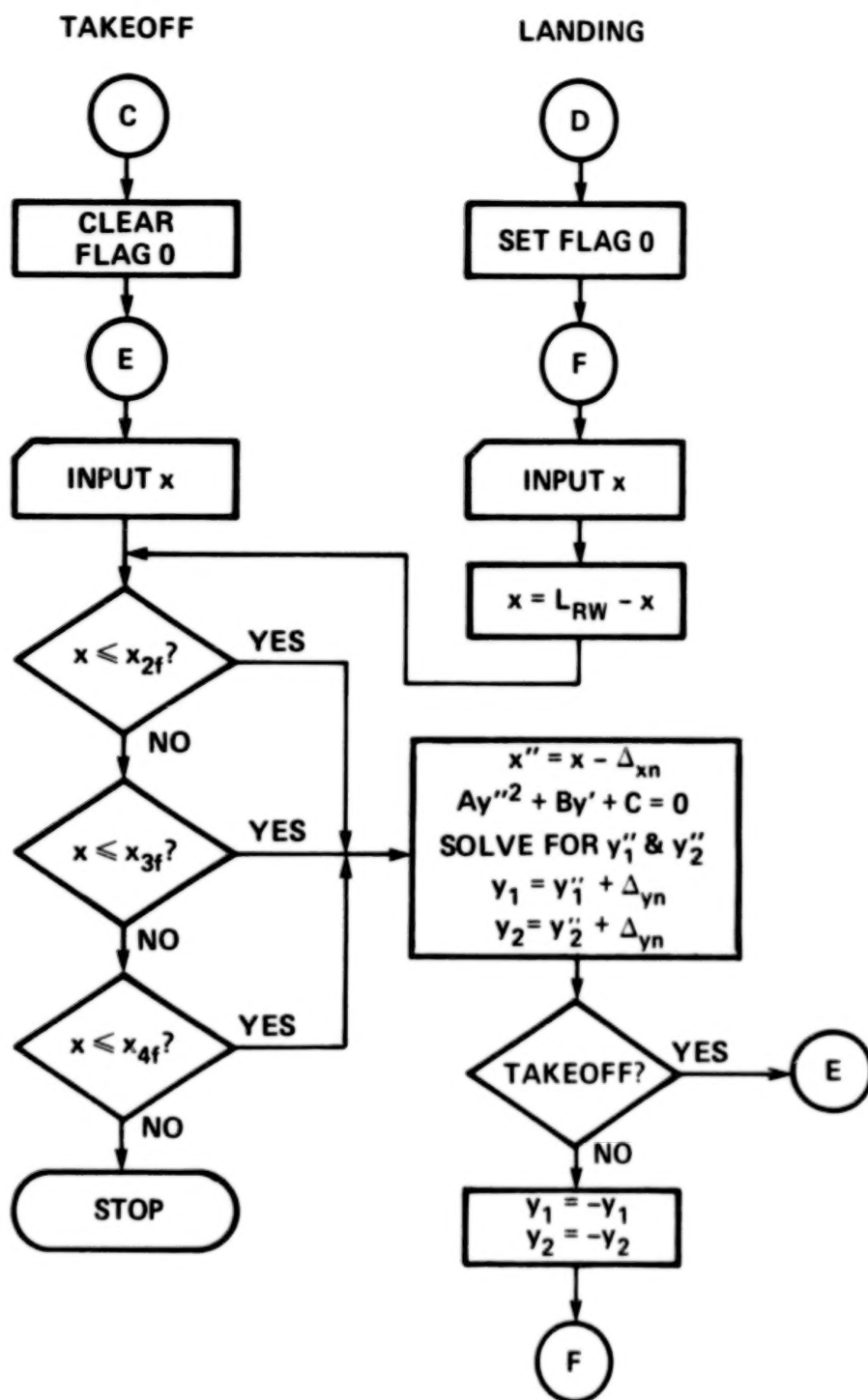


Figure 6.- Flow chart of contour-plotting program.

STEP	KEY ENTRY	KEY CODE	COMMENTS	STEP	KEY ENTRY	KEY CODE	COMMENTS												
001	LBLC				1														
	CF0				+		$d = -\sin^2 \psi_n \cos^2 \gamma_n + 1$												
	R/S				ENT↑		$A = d$												
	STO4			060	R↓														
	LBL5				÷														
	SPC				2														
	PRTX				÷														
	RCLD		x_{\max} seg 4		CHS														
	RCLC		x_{\max} seg 3		ENT↑														
010	RCLB		x_{\max} seg 2		X ²														
	RCL4		x		R↓														
	GSBa				R↓														
	RCLi				x↔y														
	TAN ⁻¹			070	÷		C/A												
	COS				STO0														
	X ²				-														
	CHS				√X		$D = [B^2/4A^2 - C/A]^{1/2}$												
	STO0				+		$y_1'' = -B/2A + D$												
	ISZI				ST=0		$y_2'' = C/y_1 A$												
020	RCLi				RCL0														
	COS				ISZI														
	STO1				GSBb		$y_1 = y_1'' + \Delta_{yn}$												
	LSTX				x↔y														
	SIN			080	GSBb		$y_2 = y_2'' + \Delta_{yn}$												
	STO2				F0?														
	X				GTOD		landing												
	X		$b = -\sin \psi_n \cos \psi_n \cos^2 \gamma_n$		GTOC		takeoff												
	ISZI				LBLa		This routine												
	RCLi				x<y?		checks to see in												
030	STO3				GTO1		which segment x												
	R↓				x↔y		lies. It checks												
	ISZI				R↓		segments 2, 3 & 4												
	RCL4				x<y?		If it is not contained												
	RCLi			090	GTO2		in either, the												
	-				x↔y		program stops												
	STO4		$x'' = x - \Delta_{xn}$		R↓														
	X				x<y?														
	2				GTO3														
	X		$B = 2bx''$		R/S														
040	RCL1				LBL1		Segment 2												
	X ²				6														
	RCL0				GTO4		Segment 3												
	X				LBL2														
	1			100	1														
	+		$a = -\cos^2 \psi_n \cos^2 \gamma_n + 1$		1														
	RCL4				GTO4		Segment 4												
	X ²				LBL3														
	X				1														
	RCL3				6														
050	X ²				LBL4														
	-				STOI														
	x↔y		$C = ax''^2 - R_n^2$		RTN														
	RCL2				LBLb		This routine computes												
	X ²			110	RCLi		$y = y'' + \Delta_{yn}$												
	RCL0				+														
	X				F0?		Takeoff or landing?												
REGISTERS																			
0	$-\cos^2 \gamma_n$	1	$\cos \psi_n$	2	$\sin \psi_n$	3	ψ_n	4	x	5	x''	6	$\tan \gamma_2$	7	ψ_2	8	R_2	9	Δ_{xn}
S0	Δ_{yn}	S1	$\tan \gamma_3$	S2	ψ_3	S3	R_3	S4	Δ_{xn}	S5	Δ_{yn}	S6	$\tan \gamma_4$	S7	ψ_4	S8	R_4	S9	Δ_{xn}
A	Δ_{yn}	B	x_{2f}	C	x_{3f}	D	L_n	E	L_{RW}	I									

Figure 7.- Code for contour-plotting program.

Figure 7.- Concluded.



Figure 8.- Noise characteristics for example conventional jet transport.

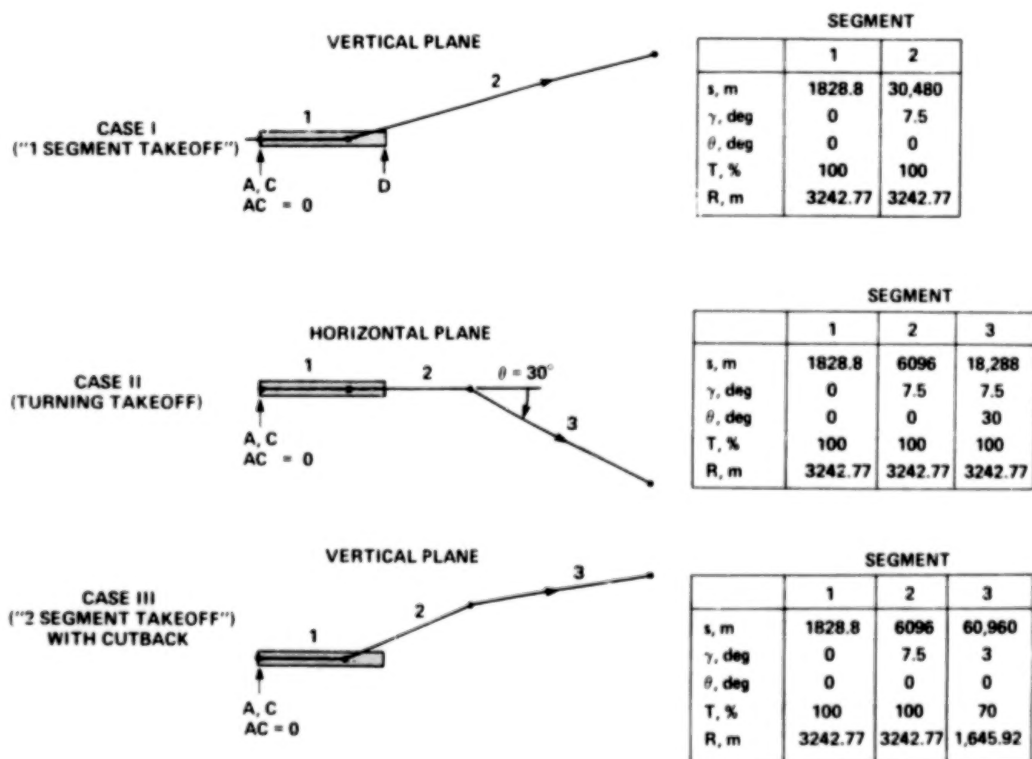
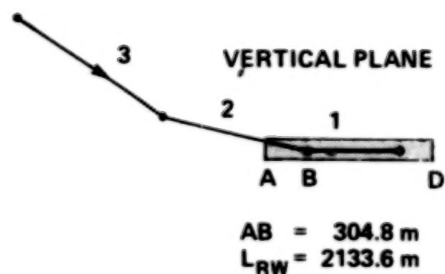


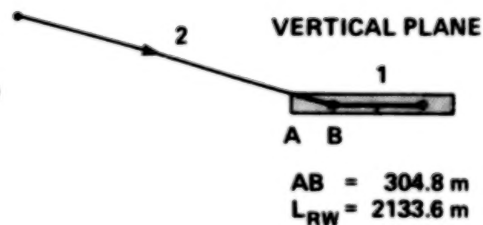
Figure 9.- Takeoff examples.

CASE IV
("2 SEGMENT LANDING")



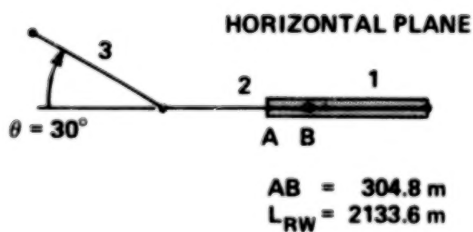
SEGMENT			
	1	2	3
s, m	1,219.2	6,096	19,812
γ , deg	0	3	7.5
θ , deg	0	0	0
T, %	45	45	45
R, m	837.83	837.83	837.83

CASE V
("1 SEGMENT LANDING")



SEGMENT		
	1	2
s, m	1,219.2	25,908
γ , deg	0	3
θ , deg	0	0
T, %	45	45
R, m	837.83	837.83

CASE VI
(TURNING LANDING)



SEGMENT			
	1	2	3
s, m	1828.8	6096.0	18,288
γ , deg	0	7.5	7.5
θ , deg	0	0	30
T, %	100	100	100
R, m	3242.8	3242.8	3242.8

Figure 10.- Landing examples.

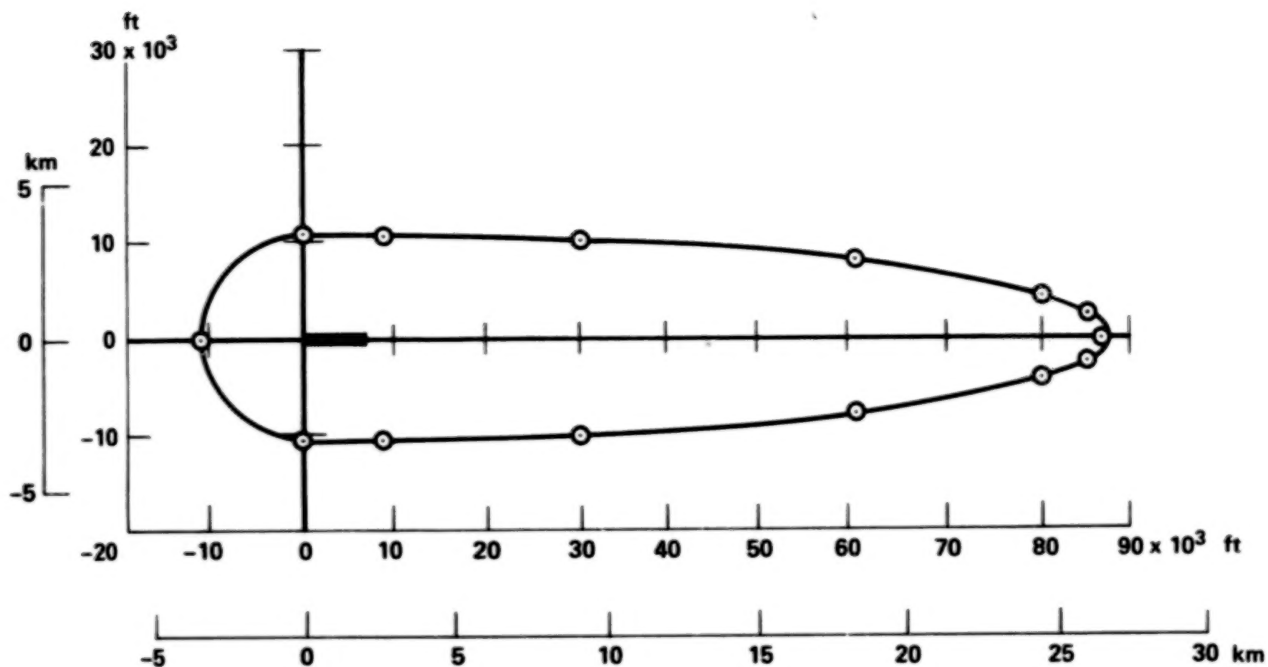


Figure 11.- Takeoff contour for Case I.

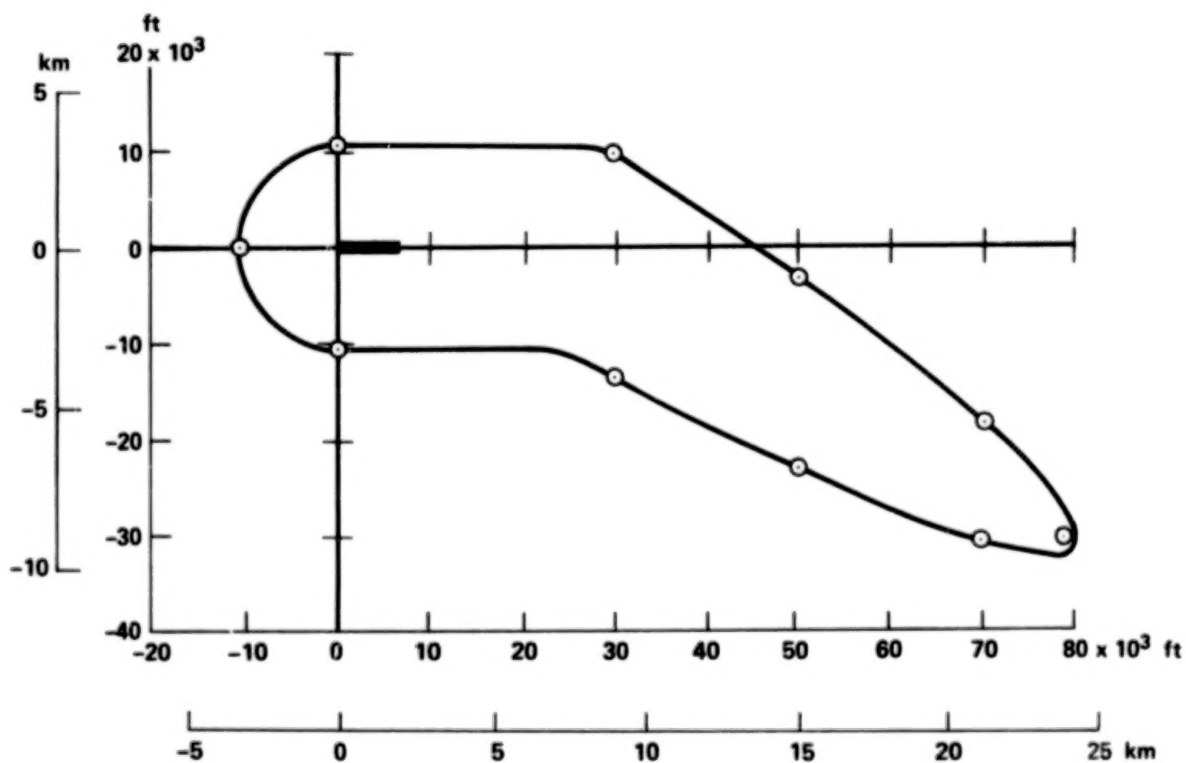


Figure 12.- Takeoff contour for Case II.

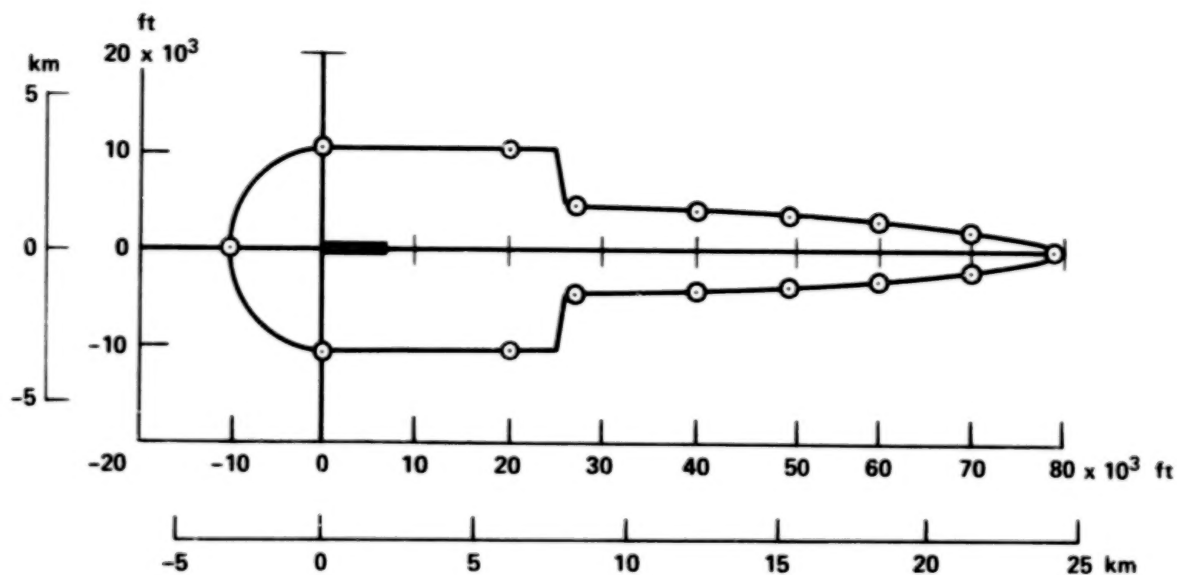


Figure 13.- Takeoff contour for Case III.

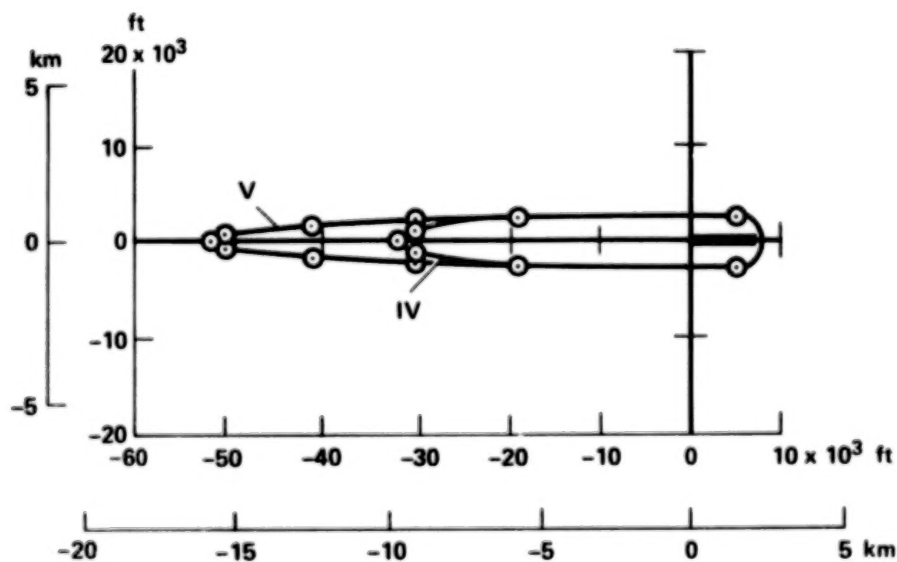


Figure 14.- Landing contour for Cases IV and V.

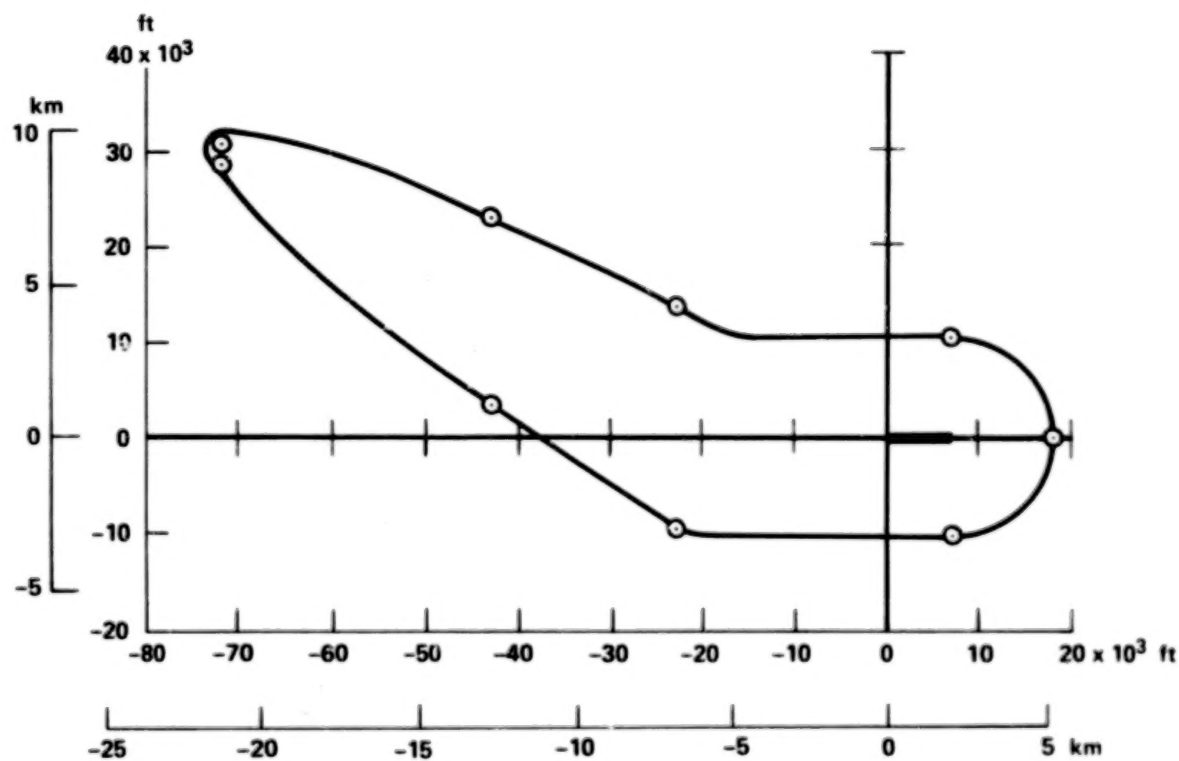


Figure 15.- Landing contour for Case VI.

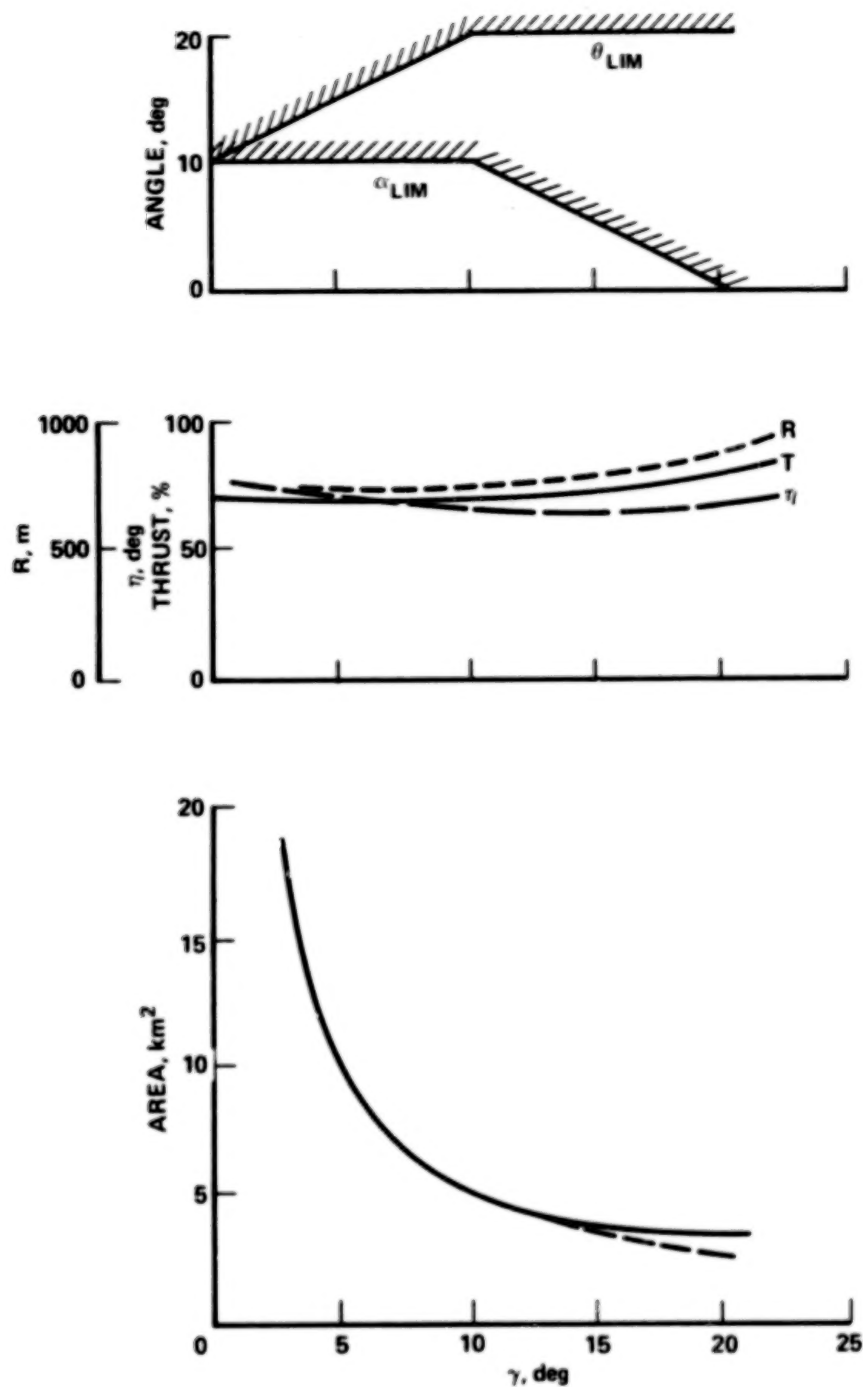


Figure 16.- Effect of flight-path angle on minimum noise footprint area for example jet STOL aircraft.

1. Report No. NASA TP-1432		2. Government Accession No.		3. Recipient's Catalog No.	
4. Title and Subtitle A CLOSED-FORM SOLUTION FOR NOISE CONTOURS				5. Report Date November 1979	
				6. Performing Organization Code	
7. Author(s) Elwood C. Stewart and Thomas M. Carson				8. Performing Organization Report No. A-7660	
9. Performing Organization Name and Address Ames Research Center, NASA Moffett Field, Calif. 94035				10. Work Unit No. 505-07-31	
				11. Contract or Grant No.	
12. Sponsoring Agency Name and Address National Aeronautics and Space Administration Washington, D. C. 20546				13. Type of Report and Period Covered Technical Paper	
				14. Sponsoring Agency Code	
15. Supplementary Notes					
16. Abstract <p>In this report is described an analytical approach for generating noise contours that overcome the difficulties of existing programs. Although many noise-contour programs are available, they require large computers and a sustained major effort for use, are complex and slow, and are generally not desirable for interactive use for on-line piloted-simulator use. The method developed here is valid for arbitrarily complex paths and reveals the importance of various factors that influence contour shape and size. The calculations are simple enough to be implemented on a small, hand-held programmable calculator, and a program for the HP-67 calculator is illustrated. The method is fast, simple, and gives the area, the contour, and its extremities for arbitrary flight paths for both takeoffs and landings.</p>					
17. Key Words (Suggested by Author(s)) Aircraft noise impact Noise impact prediction				18. Distribution Statement Unlimited STAR Category - 71	
19. Security Classif. (of this report) Unclassified		20. Security Classif. (of this page) Unclassified		21. No. of Pages 37	
				22. Price* \$4.00	

END

June 18, 1981